SURFACE CHARACTERIZATION OF CHEMICALLY MODIFIED WOOD: DYNAMIC WETTABILITY[1]

John Z. Lu†*

Postdoctoral Research Associate

and

Qinglin Wu†

Roy O. Martin Sr. Professor
School of Renewable Natural Resources
Louisiana State University Agricultural Center
Baton Rouge, LA 70803-6202

(Received July 2005)

ABSTRACT

Dynamic wettability of chemically modified yellow-poplar veneer was investigated with sessile water droplets in this study. Dynamic contact angle, decay ratio, spreading ratio, and their changing rates (the wetting slope and *K* value) were used to illustrate the dynamic wetting process. Dynamic contact angle (θ) and droplet height decay ratio (DR_h) followed the first order exponential decay equation, whereas the droplet base-diameter spreading ratio (SR_ϕ) fitted the *Boltzmann* sigmoid model. Wetting behavior of Epolene G-3015 [a maleated polypropylene (MAPP) copolymer with a high molecular weight]-treated wood surface was independent of the retention and wetting time. The retention effect on wetting slopes of θ, DR_h, and SR_ϕ on poly(ethylene and maleic anhydride) (PEMA)-treated specimens was opposite to that on Epolene E-43 (a MAPP copolymer with a low molecular weight)-treated specimens. Based on these two models, the wetting slope and *K* value were used to interpret the kinetics of wetting. Therefore, these methods were helpful to characterize the dynamic wettability of wood surfaces modified with different coupling agents.

Keywords: Chemical modification, contact angle, decay and spreading ratios, dynamic wettability, kinetics of wetting, wetting models, yellow-poplar veneer.

INTRODUCTION

Chemical modification of wood has been widely used in the manufacture of wood-polymer composites (WPC) to make the polar wood materials more compatible to the nonpolar thermoplastic polymers (Woodham et al. 1984; Dalväg et al. 1985). As one of the most popular chemical modification methods, coupling treatments effectively improve the compatibility between the wood and polymeric matrix and the interfacial bonding strength of the resultant composites. Most effective coupling forms at the interface in WPC are usually created through the interfacial similarity rule (Lu et al. 2000). Coupling treatments either make the polymer matrix have polar surfaces or make the wood surfaces less polar. The latter method is more efficient and has been extensively applied in WPC. The interfacial similarity rule is the basis for improving the interfacial compatibility and adhesion in WPC (Lu et al. 2000).

In general, the interfacial wettability requirement in WPC is opposite to that for traditional wood composites. In WPC, the modified wood surfaces are required to have a smaller surface

[1] This paper is published with the approval of the Director of Louisiana Agricultural Experiment Station.

† Member of SWST.

* Current address for John Z. Lu: Department of Wood Science and Engineering, 142 Richardson Hall, Oregon State University, Corvallis, OR 97331-5751

energy (i.e., larger contact angles) in order to improve their compatibility with thermoplastics. In wood composites, the adhesive resins should have smaller contact angles on wood for better wetting and adhesion. Although a number of research articles on dynamic wetting process for wood adhesion have been published (Scheikl and Dunky 1998), there have been few reports on the dynamic wetting process in WPC. In an earlier study (Lu and Wu 2005), the morphology of water droplets on wood veneer with different coupling agents was investigated. The study showed that coupling agent type, molecular structure, and retention greatly influenced the wetting behavior of the modified wood surfaces and wood-polymer interface. Moreover, the contact angle and profile dimension of water droplets were related to the wetting time. However, the time-dependent wetting process in WPC was not fully understood. Hence, it is necessary to further study the characteristics of the dynamic wetting process for chemically modified wood surfaces and wood-polymer interface.

The objective of this study was to investigate the dynamic wettability of wood surfaces modified with different coupling agents. The contact angle of water droplets and time-dependent changes in their profile dimension (e.g., base-diameter and height) were measured and modeled. Based on the geometrical changes of the water-droplet profile, the wetting slope and K value were derived to illustrate kinetics of wetting, and therefore evaluate the dynamic wettability of the modified wood surfaces.

BACKGROUND

Contact angle analysis in wood-polymer composites

As early as 1976, Young (1976) investigated the wettability of wood pulp fibers grafted with styrene and acrylonitrile monomers using the Wilhelmy technique (Wilhelmy 1863). The modified fibers presented different wetting characteristics. Acrylonitrile-grafted fiber had a wetting behavior similar to the untreated fibers. However, the styrene-grafted fiber had a reduced wettability (i.e., a larger static contact angle and smaller surface energy) with respect to the ungrafted fiber (Young 1976).

Little attention had been paid to the wettability at the interface in wood-polymer composites until the 1990s. Felix and Gatenholm (1991) investigated the wettability of wood fibers treated with maleated polypropylene (MAPP). They reported that static contact angle of cellulose fibers treated with MAPP was in the range of 130° and 140°. There was no significant difference of static contact angle between the specimens extracted and unextracted with toluene before coupling treatment. Chen et al. (1995) studied the adhesion properties of styrene-lignin graft copolymers using a Cahn dynamic contact angle (DCA) analyzer. The static contact angle data measured with distilled water on grafted lignin were close to those of polystyrene (i.e., 105°).

Gardner et al. (1994) used the DCA and micro-bond technique to evaluate the interfacial adhesion in wood fiber-polystyrene composites. They reported that contact angles of water on wood fibers treated with styrene-maleic anhydride (SMA) copolymers increased with the grafting weight percent gain. However, the increase of SMA acid number resulted in the decrease of contact angle for SMA-treated specimens.

Matuana et al. (1998) used four different coupling agents to treat the wood veneer and investigated the wettability of the chemically modified wood specimens. For the specimens treated with anhydride-based coupling agents (such as Epolene E-43 and phthalate anhydride), the initial contact angles of glycerol sessile drops on treated wood were in the range from 100° to 110°. Based on the relationship between the exposure time and contact angles, the wetting behaviors of the modified specimens showed that coupling treatment helped improve the compatibility at the interface.

More recently, the influence of maleation on the polymer adsorption and fixation, wood surface wettability, and interfacial bonding strength in wood-PVC composites was studied (Lu et al. 2002). Veneer specimens treated with two MAPPs (Epolene G-3015 and Epolene E-43)

presented different wetting behavior. For G-3015-treated specimens, the measured static contact angle varied from 115°-130°, independent of the retention, graft rate, and wetting time. For E-43-treated samples, the retention, graft rate, and wetting time had a significant influence on the static contact angle. After removing the ungrafted or non-reacted maleic anhydride (MA) groups in grafted E-43 on the wood sample, the static contact angle decreased with an increase in the graft rate and wetting time because many hydrolyzed products of free MA groups (double or single carboxylic groups) on grafted E-43 molecular chains were released and freely exposed on the wood surfaces during wetting. Consequently, the wettability of maleated wood specimens was mainly influenced by the acid number of coupling agents, amount of free MA groups, and surface polarity.

Theoretical modeling of the dynamic wetting process

When a probe liquid (e.g., water and urea- or phenol-formaldehyde resin) is placed on the wood, it spreads on the surface. Simultaneously, it penetrates into the wood and is gradually absorbed by the wood through capillary action (Fig. 1). The absorption may accompany the evaporation of water molecules into the atmosphere by a surface tension. During wetting, the droplet expands in the contact area under the surface tension (this process is defined as *spreading*), whereas it shrinks in the height and volume by penetration, evaporation of water, and spreading (this process is defined as *decaying*). The dynamic wetting process is not completed until the wood substrate is completely wetted.

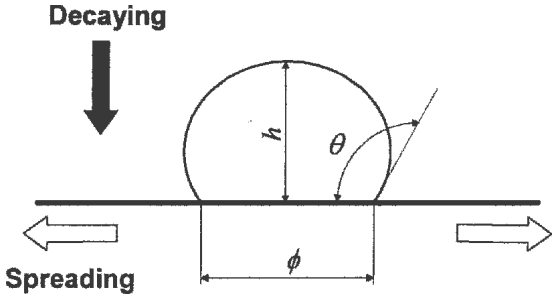

FIG. 1. Profile of a probe liquid on wood veneer.

Several models have been proposed to describe the dynamic wetting process (Chen 1972; Liptáková and Kúdela 1994; Liu et al. 1995; Shi and Gardner 2001). Among these models, a natural decay model in nuclear physics (Halliday et al. 1997) was used to characterize the decay process for a sessile water droplet. The model has the following form:

$$\theta = \theta_0 + a \cdot \exp(-K_\theta t) \quad (1)$$

where, θ_0 = initial contact angle, degrees,
θ = contact angle at time, t, degrees,
t = wetting time, seconds,
K_θ = K value in θ,
a = a material constant.

Equation (1) can be expressed in a natural logarithmic form (Elliott and Ford 1972). Hence, the dynamic wetting process of water droplets on the modified surface follows the first-order kinetic law (Wolstenholme and Schulman 1950). Similarly, the droplet height (h) and volume (V) follow the same process as a function of the wetting time. Thus, Eq (1) also applies to the decay process of h and V.

For the spreading process, the *Boltzmann* equation was applied to simulate the dimensional changes in the base-diameter (ϕ), perimeter (ρ), and contact area (S) of a droplet during dynamic wetting. The equation is expressed as follows (Devanne et al. 1997):

$$\delta = \frac{\delta(+\infty) - \delta(-\infty)}{1 + \exp[(t_0 - t)/\Delta t]} + \delta(-\infty) \quad (2)$$

where, δ = the dimensional size in ϕ, ρ, or S, mm or mm^2 at time t,
$\delta(-\infty)$ = the initial value of dimension, mm or mm^2,
$\delta(+\infty)$ = the final value of dimension, mm or mm^2,
t_0 = the time at which δ is equal to the average of $\delta(-\infty)$ and $\delta(+\infty)$, seconds, and
Δt = interval of time t, seconds,

In order to compare the influence of the exponential term on the dynamic wetting process, Eq. (2) can be rewritten as:

$$\delta = \frac{\delta(+\infty) - \delta(-\infty)}{1 + c \cdot \exp(-K_\delta t)} + \delta(-\infty) \qquad (3)$$

where c is a material constant. The K values (e.g., K_θ and K_δ) in Eqs. (1) and (3) are a scale parameter. The slopes of curves for θ, h (or V) and ϕ (or ρ and S) at time t are derived from Eqs. (1) and (3) by differentiation with time t, respectively, and defined as the wetting slopes (WS). They are labeled as WS_θ for the contact angle, WS_h for the droplet height, and WS_ϕ for the droplet base-diameter, respectively. Shi and Gardner (2001) suggested using the K values to quantify the spreading and penetration rates. In this study, the K values describe the shape of the decay and spreading models (Eqs. 1 and 3), while the wetting slopes are used for the wetting speeds.

MATERIALS AND METHODS

Test materials and sample preparations

Two maleated polypropylene (MAPP) copolymers (Epolenes E-43 and G-3015, Eastman Chemical Company) and one poly[maleic anhydride and ethylene (with a 1:1 molar ratio)] copolymer (PEMA, Polysciences, Inc.) were used in this study. PEMA can be classified as a carboxylated polyolefin. The properties of these coupling agents are listed in Table 1. Benzoyl peroxide (BPO, Aldrich) was used as an initiator. Toluene (Fisher Scientific) was used as a solvent for both MAPPs and propanol (Fisher Scientific) for PEMA.

Polyvinyl chloride (PVC) sheets (508 mm × 1270 mm × 0.0508 mm) were purchased from Curbell Plastics Company, Phoenix, AZ. Each PVC specimen was cut into 50.8 mm × 25.4 mm in size prior to use.

Sheets of commercial yellow-poplar (*Liriodendron tulipifera*) veneers (610 mm × 610 mm) were obtained from Columbia Forest Products Inc., Newport, VT. The nominal thickness for yellow-poplar was 0.91 ± 0.127 mm. Each veneer specimen was cut into 50.8 mm × 25.4 mm in size from the veneer sheets. Before coupling treatments, all veneer specimens were conditioned to 5% moisture content (MC) in a conditioning chamber.

Soxhlet extraction

Soxhlet extraction was conducted on all wood specimens according to the ASTM standard D1105-96 (ASTM 1998) to reduce the influence of extractives on chemical coupling. Wood samples were first extracted with a 120-ml mixing solution of toluene and ethyl alcohol for 4 h. They sequentially underwent the second extraction with 120 ml ethyl alcohol for 4 h (Lu et al. 2002). The extracted wood specimens were finally oven-dried at 70°C to reach a constant weight. The oven-dried weight of each sample was measured.

Coupling treatments

Wood specimens were dipped in coupling solution at 100°C for 5 min under continuous stirring with a magnetic stirrer (Lu et al. 2002). The concentration levels of coupling agent were de-

TABLE 1. *Properties of coupling agents.*

Coupling agent[a]	Shape and appearance	Density (g/ml)	Molecular weight[b] (g/mol)		Acid number (mgKOH/g)	Estimated amount of function groups (wt %)	Viscosity (Pa s)[c]
			$\overline{M}_w$	$\overline{M}_n$			
E-43	Yellow pellet	0.93	9,100	3,900	47	4.9	0.4
G-3015	Light yellow pellet	0.91	47,000	24,800	15	1.6	25
PEMA	White flour	–	100,000	–	870	69.9	0.005

[a] The pH value of 5% PEMA solution at 20°C is 5.20.
[b] $\overline{M}_w$ and $\overline{M}_n$ represented the weight and number average molar masses, respectively.
[c] The viscosity values for E-43 and G-3015 were measured at 190°C. The viscosity of PEMA was measured in 2% solution.

signed to be 12.5, 25, 50, and 75 g/L. The weight ratio between the BPO and coupling agent was 0.5. The treated specimens were removed from the solution and cooled to room temperature. All modified specimens were oven-dried at 70°C to reach a constant weight for calculation of coupling agent retention. The coupling agent retention was determined based on the weight percentage of the fixed coupling agent on a modified wood specimen (Lu et al. 2002). Before the contact angle measurement, all modified specimens were conditioned to about 5% MC.

Measurements of contact angle and water droplet profile

An imaging system was used for the contact angle and profile measurements on the modified wood veneer. This system consisted of a microscope, a CCD camera, a fiber optic illuminator, a signal transfer, a monitor for zooming images, and a computer (Lu 2003; Lu and Wu 2005). During measurement, a specimen was placed on the top of a miniature view-station in front of the microscope with a CCD video camera. For all specimens, the measurements were conducted at 24 ± 1°C and a relative humidity (RH) of 50%.

A 10-μl distilled water droplet was placed on the specimen surface with a micropipette. Three replications were used for each specimen. The position of a droplet on a specimen was adjusted horizontally until it was clearly focused on the zooming monitor (Lu and Wu 2005). The images of the droplet were taken as a function of time and stored as image files with Kodak Imaging® software for further processing. The base-diameter of the droplet on each specimen was measured at 0, 5, 15, 30, 60, 90, and 120 s after it fell down on the wood surface. The contact angle and droplet height from the images were measured at 0, 3, 5, 10, 15, 20, 30, 45, 60, and 100 (Fig. 1).

In this study, all contact angle measurements were conducted along the wood grain direction. The contact angle and profile dimensions were measured with SigmaScan Pro5® software. For each image, the profile dimensions and contact angles at each time interval were measured four times, respectively. The average values with a standard deviation value less than 1.0 were taken as a set point for each image.

Data modeling

The experimental data were modeled using Eq. (1) and (3). In order to describe the decay and spreading processes more precisely, a decay ratio (*DR*) for *h* or *V* and spreading ratio (*SR*) for ϕ, ρ, or *S* were defined as:

$$DR_h \text{ or } SR_\phi = \frac{\Gamma(t)}{\Gamma(0)} \tag{4}$$

where, Γ = *h* or ϕ,

$\Gamma(t)$ = the dimensional size of a droplet profile at *t* seconds, and

$\Gamma(0)$ = the dimensional size of a droplet profile at 0 second.

During the model fitting, *DR* and *SR* were calculated as a function of time. Similarly, the wetting slopes of *DR* and *SR* for *h* and ϕ are defined as WS_{DRh} and $WS_{SR\phi}$, respectively. In this study, the retention levels and θ, DR_h, and SR_ϕ values were accurate to one decimal figure, while the *K* and WS values were kept as three effective decimals.

GrandPad Prism® software (Motulsky 1999) was used to fit the data through nonlinear regression. The first-order exponential decay model (Eq. 1) and the *Boltzmann* sigmoid (Eq. 3) from the Prism Equation Library were selected with a 95% confidence interval to fit the data set. After fitting, a graph of residuals (i.e., the distances of each point from the curve) was plotted to check the goodness of fit. The maximum residual was made to be as small as possible for the best fit.

RESULTS AND DISCUSSION

Dynamic contact angle

As shown in Fig 2, wood veneers treated with these three coupling agents presented different wetting behavior at a close coupling agent retention level. Within 15 s, E-43-treated veneer

TABLE 2. *Kinetics of wetting for water droplets on PVC and the unmodified and modified yellow-poplar veneer specimens.*

Material	Coupling agent retention (%)	Contact angle (θ)[a,b,c]			Decay ratio in height (DR_h)[a,b,c]			Spreading ratio in base-diameter (SR_θ)[a,b,c]		
		K_θ	$WS_\theta(0)$	$WS_\theta(15)$	K_{DRh}	$WS_{DRh}(0)$	$WS_{DRh}(15)$	$K_{SR\theta}$	$WS_{SR\theta}(0)$	$WS_{SR\theta}(15)$
PVC	0	0.0553	−0.278	−0.121	0.0105	−0.000920	−0.000785	4.313	−0.00677	0
Wood	0	0.0189	−1.755	−1.323	0.0145	−0.00811	−0.00652	0.0191	0.0252	0.0207
E-43-treated veneer	2.9	1.049×10^{-5}	−0.563	−0.563	2.551×10^{-6}	−0.00330	−0.00330	0.0151	0.000574	0.00695
	4.1	0.0854	−8.788	−2.440	0.0763	−0.0614	−0.0196	0.0696	0.141	0.0772
	6.8	0.154	−12.836	−1.272	0.148	−0.125	−0.0135	0.0682	0.0169	0.0660
	7.4	0.0731	−6.875	−2.295	0.0465	−0.0329	−0.0164	0.0274	0.0446	0.0304
G-3015-treated veneer	2.2	0.00436	−0.0697	−0.0653	1.441×10^{-5}	−0.000211	−0.000211	0.406	0.000234	0.00146
	3.6	0.000983	−0.0243	−0.0243	0.00436	−0.000439	−0.000411	53.079	5.137×10^{-7}	0
	6.3	0.0615	−0.0867	−0.0345	2.859×10^{-5}	−0.000277	−0.000277	0.298	0.00175	2.968×10^{-5}
	10.5	0.105	−0.133	−0.0277	0.0201	−0.000433	−0.000321	21.552	0	0
PEMA-treated veneer	4.7	0.0726	−5.629	−1.894	0.0457	−0.0408	−0.0206	0.0781	0.104	0.0335
	9.5	0.0427	−2.700	−1.424	0.0298	−0.0165	−0.0106	0.0229	0.0267	0.0197
	16.1	0.0383	−2.505	−1.410	0.0285	−0.0136	−0.00885	0.0227	0.0193	0.0142
	23.9	0.268	−3.844	−0.0690	0.00921	−0.00209	−0.00182	0.0164	0.00230	0.00199

[a] K_θ, K_{DRh}, and $K_{SR\theta} - K$ values related to θ, DR_h, and SR_θ, respectively.
[b] WS_θ, WS_{DRh}, and $WS_{SR\theta}$—the wetting slopes of θ, DR_h, and SR_θ, respectively.
[c] The values in parentheses are the wetting time intervals. A negative wetting slope indicates a decreasing trend.

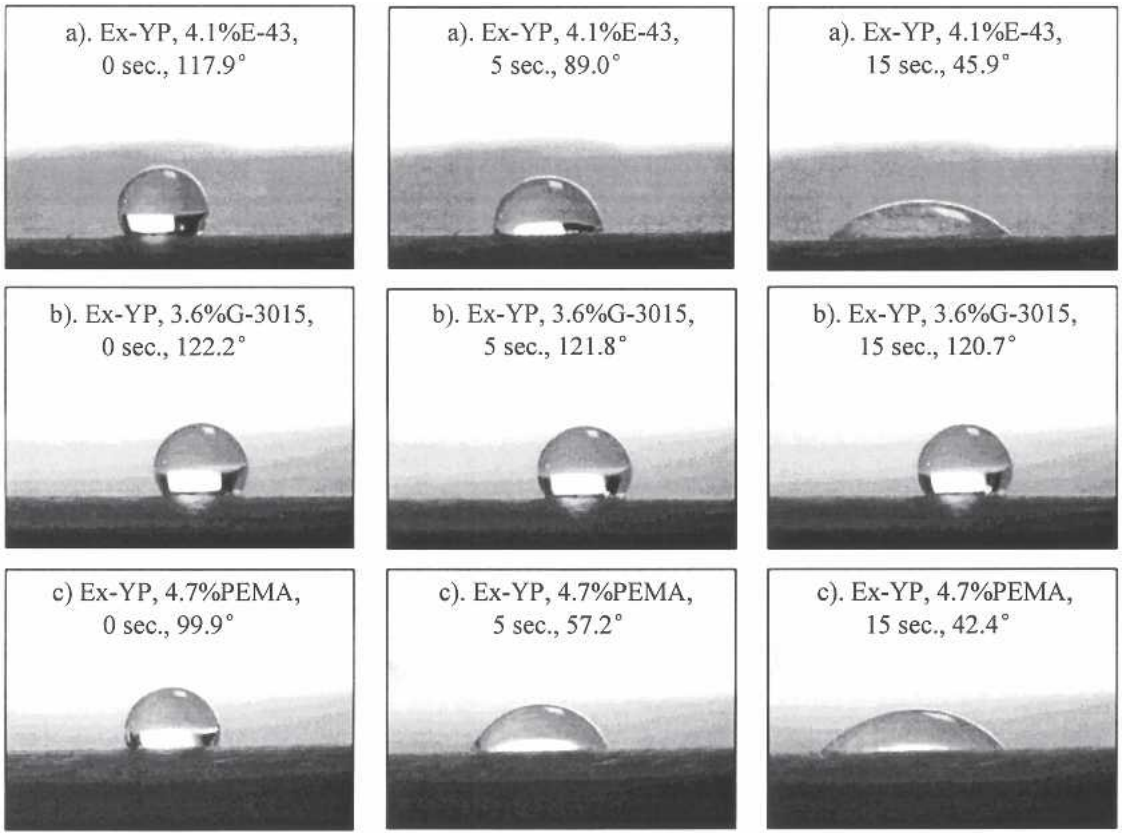

FIG. 2. Contact angle changes on the modified yellow-poplar specimens with extraction (Ex-YP) at different wetting periods. a) E-43, b) G-3015, and c) PEMA.

had a large decrease in the contact angle (> 70.0°, Fig. 2a). However, G-3015-treated veneer had few changes in the contact angle (< 2.0°, Fig. 2b). PEMA-treated specimens also had a large contact angle change (> 50.0°), similar to E-43-treated specimens (Fig. 2c).

For E-43-treated specimens, the contact angle decreased with an increase in the retention and wetting time (Fig. 3a). The contact angle had a small decrease at low retention but a large drop at high retention. The largest contact angle drop occurred at the 6.8% retention level.

The contact angle on G-3015-treated veneer was independent of the retention and wetting time. At each retention level, the contact angle on G-3015-treated surfaces was almost a constant in the wetting period between 0 and 100 s (Fig. 3b).

For PEMA-treated veneer, the measured contact angle had a large drop at low retention but a small decrease at high retention. The contact angle drop decreased with an increase in the retention (Fig. 3c). At the 4.7% level, the contact angle decreased by 79.5° within 45 s. At the 23.9% level, however, the contact angle had a small change within the first 10 s and leveled off at about 83.0° after 20 s.

Decay and spreading ratios

The dynamic wetting process of wood veneer modified with these coupling agents at various retention levels was characterized with the decay and spreading ratios (Figs. 4 and 5). In general, *DR* was a decreasing function of the wetting

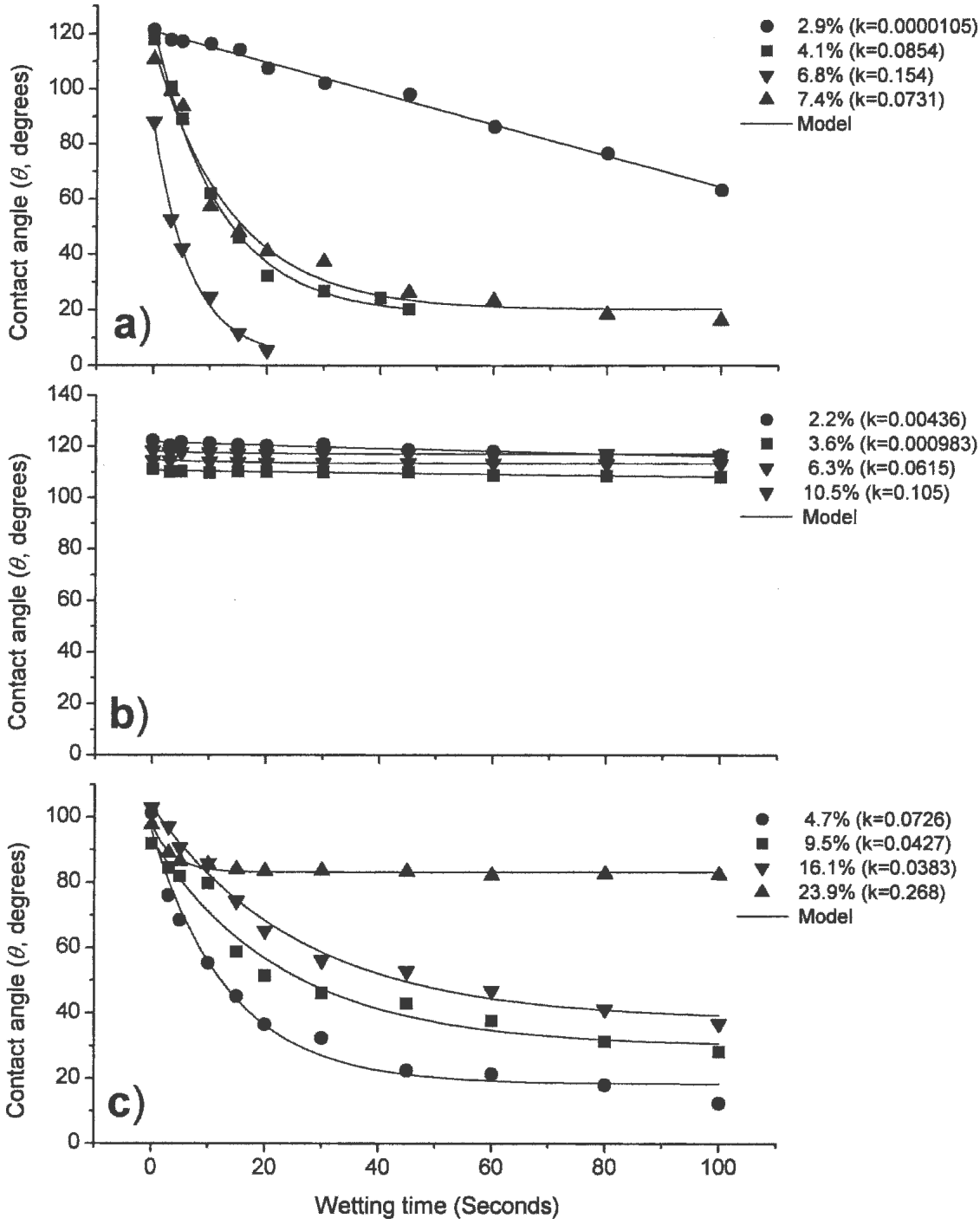

FIG. 3. Effect of the coupling agent retention on contact angle of water droplets on wood surfaces treated with a) E-43, b) G-3015, and c) PEMA.

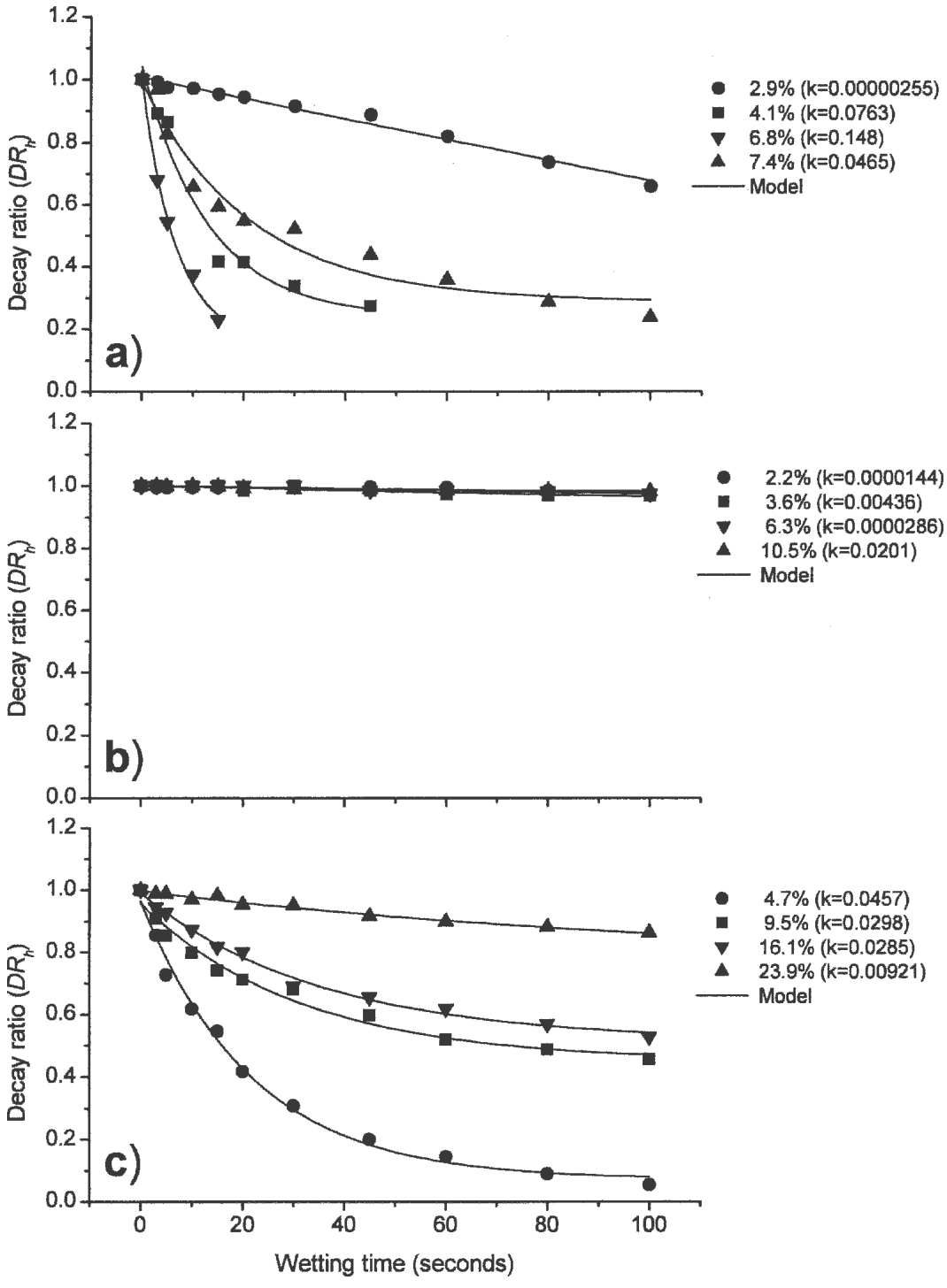

FIG. 4. Effect of the coupling agent retention on the decay ratio of water droplets on wood surfaces treated with a) E-43, b) G-3015, and c) PEMA.

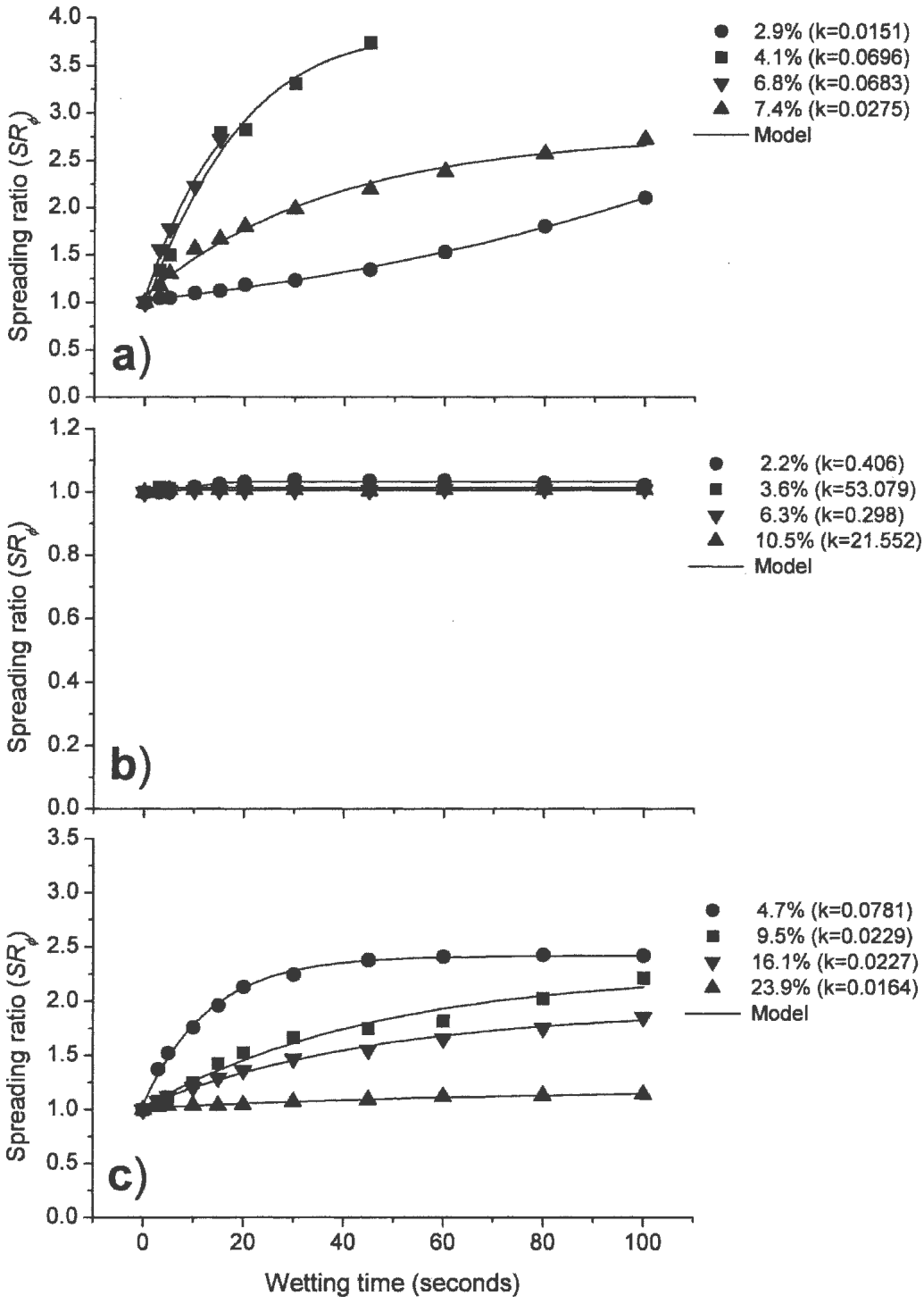

FIG. 5. Effect of the coupling agent retention on the spreading ratio of water droplets on wood surfaces treated with a) E-43, b) G-3015, and c) PEMA.

time, whereas *SR* was an increasing function of the wetting time.

For E-43-treated specimens, DR_h at the 2.9% level decreased slowly, and it had the largest drop at the 6.8% level. DR_h at the 2.9% level decreased from 1.0 to 0.7 in about 100, but it decreased by 0.8 less than 20 s at the 6.8% level. At the 7.4% level, DR_h gradually decreased and leveled off at 0.3 (Fig. 4a). However, the G-3015 retention levels had no significant influence on DR_h. As shown in Fig. 4b, DR_h on G-3015-treated veneer was close to one irrespective of the retention and wetting time. The influence of the retention on DR_h for PEMA-treated specimens was opposite to that for E-43-treated specimens. For PEMA, DR_h at the 4.7% level had the largest drop. However, DR_h at high retention (> 9.0%) gradually decreased with an increase in the wetting time (Fig. 4c). For instance, DR_h at the 23.9% level had a value between 0.9-1.0.

For E-43-treated specimens, SR_ϕ increased with an increase in the retention and wetting time (Fig. 5a). Within 100 s, SR_ϕ at the 2.9% level increased from 1.0 to 2.1, but it increased from 1.0 to 3.7 within about 45 s at the 4.1% level. However, SR_ϕ at the 7.4% level only increased from 1.0 to 2.7 within 100 s (Fig. 5a). For G-3015-treated specimens, all SR_ϕ values were close to 1.0 and independent of the retention and wetting time (Fig. 5b). For PEMA-treated specimens, SR_ϕ decreased with an increase in the retention (Fig. 5c). At the 23.9% level, however, SR_ϕ was around 1.0 and did not depend on the wetting time.

Figure 6 shows the difference in the dynamic wetting process on E-43-, G-3015-, and PEMA-treated wood specimens at the close retention levels. E-43-treated specimens had the largest SR_ϕ, while the SR_ϕ values on PEMA-treated specimens were larger than those on G-3015-treated specimens. For both E-43 and PEMA-treated specimens, DR_h was almost the same and smaller than that of the unmodified specimens (Fig. 6). At low retention (< 4%), however, DR_h on PEMA-treated specimens had a larger drop than that on E-43-treated specimens (Fig. 4). For G-3015-treated specimens, both DR_h and SR_ϕ did not depend on the retention and wetting time. They were stabilized at around 1.0, similar to those of PVC (Figs. 4b and 5b and Table 2).

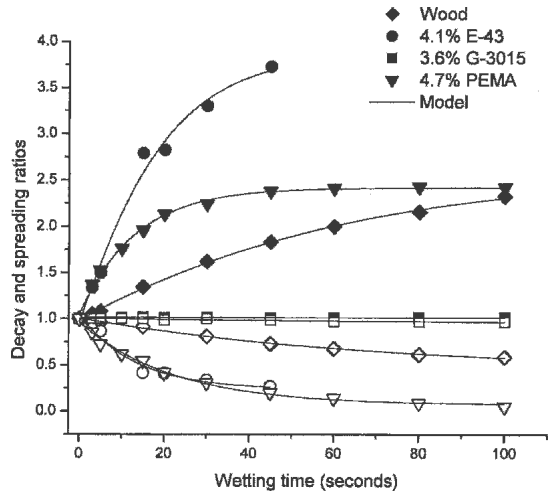

FIG. 6. Dynamic wetting behaviors of the unmodified and E-43-, G-3015-, and PEMA-treated yellow-poplar veneers. The solid symbols represent the spreading ratios in base-diameter (SR_θ), whereas the empty ones denote the decay ratios in height (DR_h).

Wetting slope

As shown in Table 2, the wetting slope of a water droplet on PVC was much smaller than that on the wood because PVC is not wetted by water. Both PVC and the wood had a negative wetting slope in the contact angle and decay ratio. Different from the wood, however, PVC had a negative wetting slope in the spreading ratio. The water droplet on PVC was gradually shrinking in volume and base-diameter due to the evaporation of water, while the droplet on the wood was spreading in the base-diameter because of the polar wood surface (Table 2). Therefore, the difference in dynamic wettability for PVC and the wood was easily determined with the wetting slopes.

For all modified wood specimens, WS_θ varied with the coupling agent type and retention (Table 2). Moreover, all wetting slopes on the modified specimens converged into zero with an increase in the wetting time (Figs. 3 to 5). E-43- and PEMA-treated specimens had a larger WS_θ

than G-3015-treated specimens. The initial wetting slope, $WS_\theta(0)$, on E-43-treated specimens increased with an increase in the retention. The slope reached −12.836 at the 6.8% level, but it went back to −6.875 at the 7.4% level. For G-3015-treated specimens, the initial wetting slope, $WS_\theta(0)$, was proportional to the retention. However, the slope at 15 s, $WS_\theta(15)$, decreased with an increase in the retention. For PEMA-treated specimens, both $WS_\theta(0)$ and $WS_\theta(15)$ decreased with an increase in the retention.

E-43- and PEMA-treated specimens had a larger initial slope, $WS_{DRh}(0)$, and a larger slope at 15 s, $WS_{DRh}(15)$, than G-3015-treated specimens. For E-43 treated specimens, the slopes $WS_{DRh}(0)$ and $WS_{DRh}(15)$ increased with an increase in the retention. $WS_{DRh}(0)$ reached its maximum value at the 6.8% level, but $WS_{DRh}(15)$ had a maximum value at the 7.1% level (Table 2). However, the wetting slopes on PEMA-treated specimens decreased with an increase in the retention. On G-3015-treated specimens, both $WS_{DRh}(0)$ and $WS_{DRh}(15)$ were equal to or close to zero, independent of the retention and wetting time.

$WS_{SR\Phi}$ had a trend similar to WS_{DRh} on the modified specimens. For example, $WS_{SR\Phi}(0)$ and $WS_{SR\Phi}(15)$ on E-43-treated specimens increased with an increase in the retention. For PEMA-treated specimens, $WS_{SR\Phi}(0)$ at the 4.7% level had a maximum value of 0.0781, but it was close to zero at the 23.9% level (Table 2).

K value

For E-43- specimens, the K values (i.e., K_θ, K_{DRh}, and $K_{SR\Phi}$) were proportional to the retention. However, the K values on PEMA-treated specimens were inversely proportional to the retention (Table 2). E-43-treated wood had a small K value at low retention, but the K values increased with an increase in the retention. However, the K value at high retention (e.g., 7.4%) decreased again. For PEMA-treated veneer, most of the K values decreased with an increase in the retention. For both decay and spreading processes, however, the K values on G-3015-treated specimens were independent of the retention levels.

Effects of coupling agents on dynamic wettability

The dynamic wettability of water droplets on the modified wood veneer was influenced by different coupling agents, because the dynamic wetting behavior of the modified wood specimens lies mainly in the structure and coupling action of coupling agents (Lu and Wu 2005). Compared with E-43, G-3015 has fewer MA groups on its molecular chains (Table 1). For G-3015, some MA groups reacted with hydroxyl groups (-OH) of lignocellulose through graft copolymerization and formed an ester linkage with the wood (Felix and Gatenholm 1991). However, some ungrafted or non-reacted MA groups may be buried in the large G-3015 molecular chains (Lu et al. 2002). Therefore, the surface of G-3015-treated veneer would be non-polar at high retention. As a result, the dynamic wettability of G-3015-treated veneer was almost independent of the retention and wetting time (Figs. 3b to 5b).

E-43 has a low molecular weight but a high acid number with respect to G-3015. Like G-3015, E-43 was grafted onto the wood through ester bridges and formed a *monolayer* structure at the interface. Graft copolymerization by E-43 is thereby limited on the layers close to wood surfaces (Lu et al. 2002). Since grafted E-43 molecular chains still contain ungrafted or non-reacted anhydride groups, these free functional groups would be released and exposed on the wood surfaces during wetting (Lu et al. 2002). At low retention (< 7.0%), E-43-treated veneer had many free MA groups with respect to G-3015-treated veneer. Hence, the polarity and wetting speed of E-43-treated veneer were proportional to the retention (Table 2 and Figs. 3a to 5a). At high retention, however, the free MA groups of E-43 easily formed the hydrogen bonds with hydroxyl groups of lignocellulose molecules by the dehydration (Felix and Gatenholm 1991), thus resulting in reduced wettability. Accordingly, the wetting slopes of θ, DR_h, and SR_Φ on E-43-treated specimens decreased at high retention (> 7.0%) due to this reduced wettability by hydrogen bonding (Figs. 3a to 5a).

As shown in Table 1, PEMA had more functional groups on its molecular chains per unit weight than E-43 and G-3015. PEMA also has the largest molecular weight among these three coupling agents. Similarly to E-43, only some carboxylic groups (-COOH) of PEMA formed an ester linkage with hydroxyl groups of lignocellulose due to the limitation of graft copolymerization at the interface. Consequently, PEMA-treated specimens had more free functional groups on the surfaces than E-43- and G-3015-treated specimens. The chemical structure of PEMA was preferred to produce hydrogen bonding between the carboxylic groups on its molecular chains and hydroxyl groups of lignocellulose and between the carboxylic groups of its molecular chains. At low retention (< 7.0%), more free carboxylic groups of PEMA were exposed on the wood surfaces. Due to the high surface polarity at low retention, PEMA-treated specimens had a large wetting slope in θ, DR_h, and SR_ϕ (Figs. 3c to 5c). At high retention (> 7.0%), however, these free carboxylic groups can easily form hydrogen bonding through intra- or intermolecular chains of PEMA and through their interaction with hydroxyl groups of lignocellulose molecules by dehydration (Lu and Wu 2005). The hydrogen bonding structure interfered with the wetting of water on the wood surfaces, thus decreasing its wetting speed on such a surface. This may be the reason that the dynamic wetting behavior of PEMA-treated veneer was opposite to that of E-43-treated veneer (Figs. 3 to 5). Hence, the dynamic wettability of the wood surfaces modified with E-43 and PEMA reflected their ability to form hydrogen bonds with the hydroxyl groups of lignocellulose and between the carboxylic groups on their intra- or intermolecular chains (Lu and Wu 2005).

Contact angle versus decay and spreading ratios

As shown in Figs. 3 to 5, DR_h and SR_ϕ quantitatively presented the decay and spreading processes, respectively. The results clearly showed that DR_h had a dynamic wetting trend similar to the contact angle (Figs. 3 and 4). Since the contact angle is proportional to the ratio of the vertical and horizontal dimensions of a droplet (i.e., the height and base-diameter), it only qualitatively reflects the dimensional changes in these two directions. The contact angle is proportional to the decay height, but is in inverse relation to the base-diameter. Based on the experimental results, the dynamic wetting process of the modified wood specimens was well presented with DR_h and SR_ϕ (Figs. 4 and 5). Moreover, both DR_h and SR_ϕ values were easily compared for various coupling agents at different retention levels (Fig. 6). Hence, these two ratios can be combined with the contact angle to better evaluate the dynamic wettability of the modified wood surfaces.

Kinetics of wetting

The wetting slope indicated the wetting speed of water droplets on the modified wood surfaces, while the K value as a scale parameter reflected the shape of a wetting curve (Table 2 and Figs. 3 to 5). Therefore, the kinetics of wetting on the modified wood specimens can be better illustrated with the combination of the K value and wetting slope.

The wetting slope varied with the retention and wetting time. A large wetting slope normally indicated a large wetting speed. For the contact angle, the unmodified and E-43- and PEMA-treated wood veneers had a larger wetting slope than PVC and G-3015-treated specimens within 15 s (Table 2). This was also true for DR_h and SR_ϕ. It was clearly shown that the wetting slopes of DR_h and SR_ϕ on PVC and G-3015-treated specimens were equal to or close to zero with respect to the non-zero wetting slopes on the unmodified and E-43- and PEMA-treated wood specimens. The large wetting speeds for E-43- and PEMA-treated wood veneer indicated the high surface polarity, whereas the small wetting speeds for G-3015-treated veneer reflected the character of a less polar or non-polar surface.

Since the wetting slope of logarithmic contact angle had a linear relationship with the wetting time (Fig. 7), it is easier to use the logarithmic

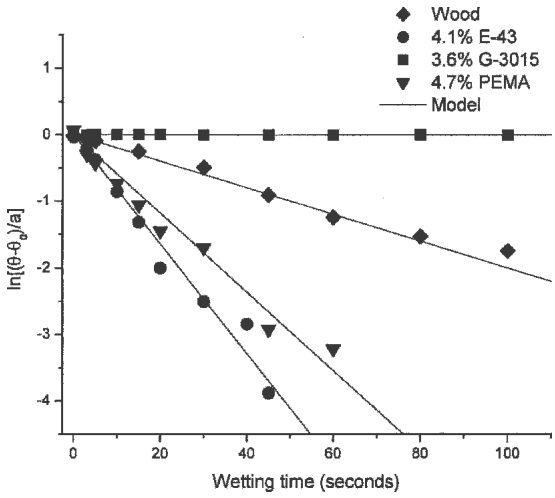

FIG. 7. Comparison on the wetting slopes of logarithmic contact angle for the unmodified and E-43-, G-3015-, and PEMA-treated wood veneers.

contact angle-wetting time plot to distinguish the dynamic wetting behavior of the modified wood surfaces. At the close retention levels, the wetting slope of logarithmic contact angle on G-3015-treated specimens was equal to or close to zero, whereas the unmodified and E-43- and PEMA-treated wood veneers had large wetting slopes. This further indicated that similar to the unmodified wood veneer, E-43- and PEMA-treated wood veneers had a higher surface energy than G-3015-treated specimens. Therefore, E-43- and PEMA-treated veneers had a hydrophilic surface, while G-3015-treated veneer had a hydrophobic surface.

For the decay and spreading processes, a large K value presented a nonlinear curve with a high curvature, while a small K value is close to a linear function. In this study, most of E-43 and PEMA-treated specimens had a nonlinear function in θ, DR_h, and SR_ϕ, while most of G-3015-treated veneer had a linear or near linear function (Figs. 3 to 5). G-3015-treated specimens had a smaller value in K_θ and K_{DRh} with respect to E-43- and PEMA-treated specimens at a close retention level (Table 2). SR_ϕ on G-3015-treated specimens varied within a small range from 1.0 to 1.1. However, G-3015-treated specimens had a large variation in $K_{SR\phi}$ with the retention. Similar to PVC (Table 2), G-3015-treated specimens had a large $K_{SR\phi}$ at the 3.6% and 10.5% levels. As shown in Fig. 5b, the spreading ratio SR_ϕ on G-3015-treated specimens had a relatively large fluctuation within the first 20 s and then gradually approached to a constant. Within this period, the corresponding K values by the *Boltzmann* sigmoid at some retention levels were sensitive to the variation of SR_ϕ. This also indicated that although G-3015-treated specimens had a reduced wettability, θ, DR_h, and SR_ϕ on G-3015-treated specimens varied in a small scale with the wetting time.

According to the kinetics of wetting, not only the surface polarity of the modified wood can be evaluated, but also the effect of coupling agent retention on the dynamic wettability in WPC can be determined. As shown in Table 2 and Figs. 3 to 5, E-43- and PEMA-treated wood veneers had a small wetting slope at high retention due to the formation of hydrogen bonds. These hydrogen bonds interfered with the coupling reaction and had a negative effect on interfacial compatibility and adhesion in WPC. Moreover, a large amount of single or double carboxylic groups at the interface may interfere with the coupling reaction at high retention levels (John 1982; Beshay et al. 1985). Although G-3015-treated wood veneer tended to have a non-polar surface at high retention, a number of G-3015 molecular chains on the wood surfaces may increase the gap between the wood and thermoplastics. For these coupling agents, therefore, a high retention level was detrimental to the interfacial compatibility and adhesion because of the decrease in the graft rate and coupling efficiency (Lu et al. 2002).

CONCLUSIONS

The dynamic wetting process of water droplets on the modified wood surfaces was described with the contact angle, decay ratio, spreading ratio, wetting slopes, and K values. For the modified wood veneer, the contact angle and decay ratio in the height followed the first-order exponential decay equation, whereas the spreading ratio in the base-diameter fitted the *Boltzmann* sigmoid model.

G-3015-treated wood had a smaller wetting slope than E-43- and PEMA-treated veneers. Most of the wetting slopes (i.e., WS_{θ}, WS_{DRh}, and $WS_{SR\Phi}$) increased with an increase in the E-43 retention, but they decreased with an increase in the PEMA retention. For G-3015-treated veneer, however, these wetting slopes were independent of the retention and wetting time. Therefore, G-3015-treated veneer presented a hydrophobic surface and acted as thermoplastics, whereas E-43- and PEMA-treated veneers had a polar surface and was more like wood in character. The K values of θ, DR_h, and SR_{Φ} were related to the curvature of a wetting function with the wetting time and described the shape of the wetting functions for the modified wood specimens. Therefore, these approaches were helpful to characterize the dynamic wettability of the modified wood surfaces and further evaluate the interfacial compatibility in WPC.

REFERENCES

American Society for Testing and Materials (ASTM) Standard. 1998. Standard test method for preparation of extractive-free wood. ASTM Standard D1105-96. West Conshohocken, PA.

Beshay, A. D., B. V. Kokta, and C. Daneault. 1985. Use of wood fibers in thermoplastic composites II: Polyethylene. Polym. Comp. 6(4):261 – 271.

Chen, C.-M. 1972. Measuring the wetting of wood surfaces by adhesives. Mokuzai Gakkaishi 18(9):451 – 456.

Chen, M.-J., J. J. Meister, D. W. Gunnells, and D. J. Gardner. 1995. A process for coupling wood to thermoplastic using graft copolymers. Adv. Polym. Technol. 14(2):97 – 109.

Dalväg, H., C. Klason, and H.-E. Strömvall. 1985. The efficiency of cellulosic fillers in common thermoplastics. Part II. Filling with processing aids and coupling agents. Int. J. Polym. Mater. 11:9 – 38.

Devanne, H., B. A. Lavoie, and C. Capaday. 1997. Input-output properties and gain changes in the human corticospinal pathway. Exp. Brain Res. 114:329 – 338.

Elliott, T. A., and D. M. Ford. 1972. Dynamic contact angles. Part 7.—Impact spreading of water drops in air and aqueous solutions of surface active agents in vapour on smooth paraffin wax surfaces. Trans. Faraday Soc. 1:1814 – 1823.

Felix, J. M., and P. Gatenholm. 1991. The nature of adhesion in composites of modified cellulose fibers and polypropylene. J. Appl. Polym. Sci. 42:609 – 620.

Gardner, D. J., F. P. Liu, M. P. Wolcott, and T. G. Rials. 1994. Improving interfacial adhesion between wood fibers and thermoplastics: A case study examining chemically modified wood and polystyrene. Pages 55–63, *in* P. R. Steiner, ed. Proc. Second Pacific Rim Bio-Based Composites Symposium, University of British Columbia, Vancouver, BC, Canada.

Halliday, D. R., R. Rensick, and J. Walker. 1997. Fundamental of physics. John Wiley & Sons, Inc., New York, NY.

John, W. E. 1982. Isocyanate as wood binders: A review. J. Adhes. 15:59 – 67.

Liptáková, E., and J. Kúdela. 1994. Analysis of the wood-wetting process. Holzforschung 48:139 – 144.

Liu, F. P., J. D. Gardner, and M. P. Wolcott. 1995. A model for the description of polymer surface dynamic behavior. Contact angle vs. polymer surface properties. Langmuir 11:2674 – 2681.

Lu, J. Z. 2003. Chemical coupling in wood-polymer composites. Doctoral dissertation, Louisiana State University, Baton Rouge, LA.

———, and Q. Wu. 2005. Surface and interfacial characterization of wood-PVC composites: Imaging morphology and wetting behavior. Wood Fiber Sci. 37(1):95 – 111.

———, ———, and H. S. MacNabb Jr. 2000. Chemical coupling in wood fiber and polymer composites: A review of coupling agents and treatments. Wood Fiber Sci. 32(1):88 – 104.

———, ———, and I. I. Negulescu. 2002. The influence of maleation on polymer adsorption and fixation, wood surface wettability, and interfacial bonding strength in wood-PVC composites. Wood Fiber Sci. 34(3):434 – 459.

Matuana, L. M., J. J. Balatinecz, and C. B. Park. 1998. Effect of surface properties on the adhesion between PVC and wood veneer laminates. Polym. Eng. Sci. 38(5):765 – 773.

Motulsky, H. 1999. Analyzing data with GraphPad Prism. GraphPad Software, Inc., San Diego, CA, http://www.graphpad.com, 1999.

Scheikl, M., and M. Dunky. 1998. Measurement of dynamic and static contact angles on wood for the determination of its surface tension and the penetration of liquids into the wood surface. Holzforschung 52:89 – 94.

Shi, S. Q., and D. J. Gardner. 2001. Dynamic adhesive wettability of wood. Wood Fiber Sci. 33(1):58 – 68.

Wilhelmy, J. 1863. Uber die Abhändigkeit der Capilaritats-Constanten des alkohols von Substanz und Gestalt des benetzten festen Köpers. Ann. Physik. 119:177 – 217.

Wolstenholme, G. A., and J. H. Schulman. 1950. Metal-monolayer interactions in aqueous systems. Part II. The adsorption of long-chain compounds from aqueous solution on to evaporation metal films. Trans. Faraday Soc. 46:488 – 497.

Woodham, R. T., G. Thomas, and D. K. Rodgers. 1984. Wood fibers as reinforcing fillers for polyolefins. Polym. Eng. Sci. 24(15):1166 – 1171.

Young, R. A. 1976. Wettability of wood pulp fibers: Applicability of methodology. Wood Fiber 8(2):120 – 128.